

## **Supplementary Materials**

### **Interpretable model of dielectric constant for rational design of microwave dielectric materials: a machine learning study**

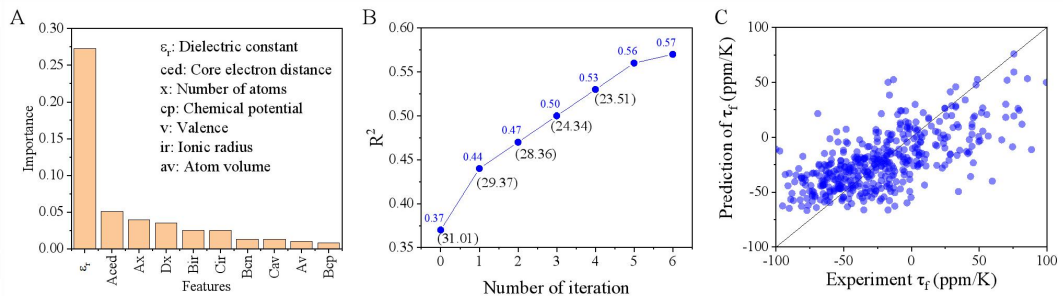
**Ye Sheng<sup>1,#</sup>, Yabei Wu<sup>1,#,\*</sup>, Chang Jiang<sup>1,#</sup>, Xiaowen Cui<sup>1</sup>, Yuanqing Mao<sup>1</sup>, Caichao Ye<sup>1,2,\*</sup>, Wenqing Zhang<sup>1,\*</sup>**

<sup>1</sup>Department of Materials Science and Engineering & Institute of Innovative Materials, Southern University of Science and Technology, Shenzhen 518055, Guangdong, China.

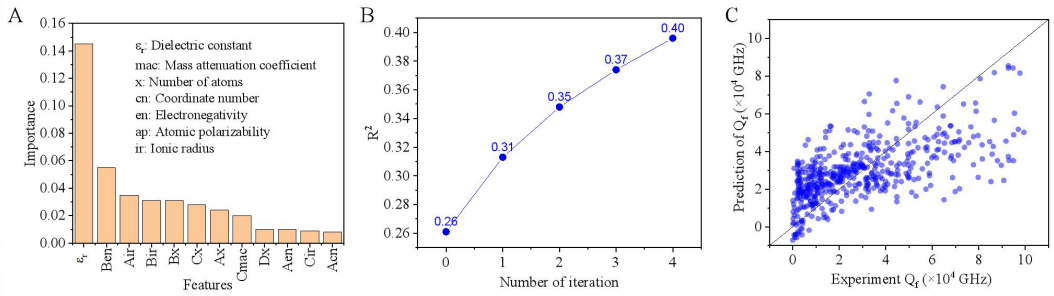
<sup>2</sup>Academy for Advanced Interdisciplinary Studies & Guangdong Provincial Key Laboratory of Computational Science and Material Design, Southern University of Science and Technology, Shenzhen 518055, Guangdong, China.

#Authors contributed equally.

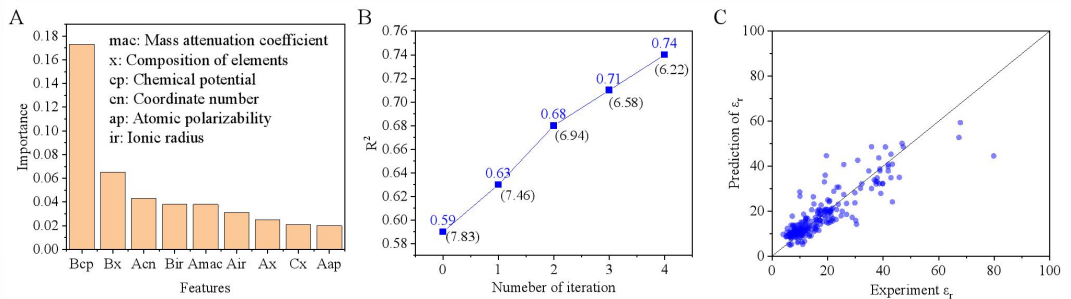
**\*Correspondence to:** Dr. Yabei Wu, Dr. Caichao Ye, Prof. Wenqing Zhang, Department of Materials Science and Engineering & Institute of Innovative Materials, Southern University of Science and Technology, No. 1088 Xueyuan Avenue, Nanshan District, Shenzhen, Guangdong 518055, China. E-mail: wuyb3@sustech.edu.cn; yecc@sustech.edu.cn; zhangwq@sustech.edu.cn



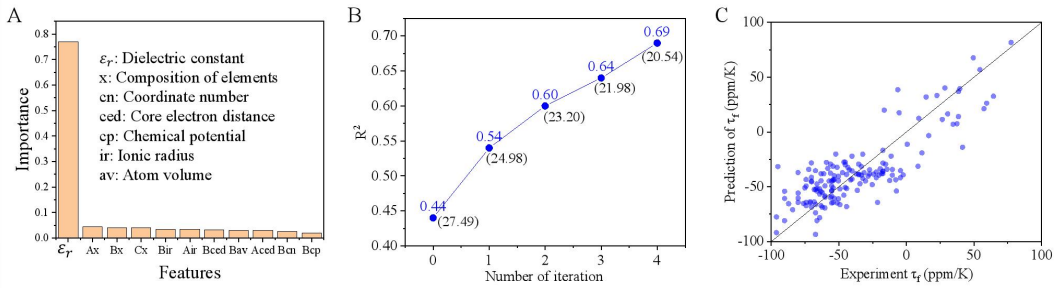
**Supplementary Figure 1.** Machine learning results of  $\tau_f$  for quaternary materials. (A) RF ranking of importance of material features for  $\tau_f$  in the quaternary materials. (B) Variation of  $R^2$  and RMSE (in the black bracket) in the prediction model of  $\tau_f$  as a function of iteration steps. (C) Scatter plot of predicted  $\tau_f$  versus experimental values for the quaternary materials after six iterations.



**Supplementary Figure 2.** Machine learning results of  $Q_f$  for quaternary materials. (A) RF ranking of importance of material features for  $Q_f$  in the quaternary materials. (B) Variation of  $R^2$  in the prediction model of  $Q_f$  as a function of iteration steps. (C) Scatter plot of predicted  $Q_f$  versus experimental values for the quaternary materials after four iterations.

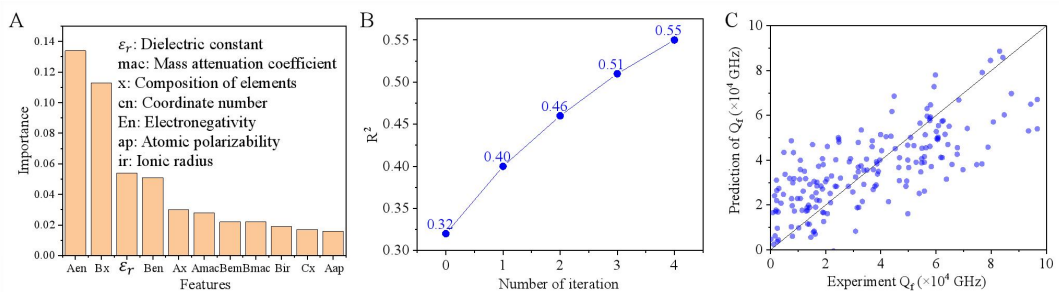


**Supplementary Figure 3.** Machine learning results of  $\epsilon_r$  for ternary materials. (A) RF ranking of importance of material features for  $\epsilon_r$  in the ternary materials. (B) Variation of  $R^2$  and RMSE (in the black bracket) in the prediction model of  $\epsilon_r$  as a function of iteration steps. (C) Scatter plot of predicted  $\epsilon_r$  versus experimental values for the ternary materials after four iterations.



**Supplementary Figure 4.** Machine learning results of  $\tau_f$  for ternary materials.

- (A) RF ranking of importance of material features for  $\tau_f$  in the ternary materials.
- (B) Variation of  $R^2$  and RMSE (in the black bracket) in the prediction model of  $\tau_f$  as a function of iteration steps.
- (C) Scatter plot of predicted  $\tau_f$  versus experimental values for the ternary materials after six iterations.



**Supplementary Figure 5.** Machine learning results of  $Q_f$  for ternary materials.

- (A) RF ranking of importance of material features for  $Q_f$  in the ternary materials.
- (B) Variation of  $R^2$  in the prediction model of  $Q_f$  as a function of iteration steps.
- (C) Scatter plot of predicted  $Q_f$  versus experimental values for the ternary materials after four iterations.

The following are the predicted models (equations) in terms of the features of quaternary and ternary materials:

### 1, Prediction model of $\varepsilon_r$ for quaternary materials:

$$\varepsilon_r = 0.164 \ln(C_{mac}) \cdot \left\{ 0.854 \cdot \frac{(C_{ap}+D_{ap}) \cdot \cos(A_x)}{C_{ap}} \cdot \left[ 0.31 \frac{C_{cp} \cdot B_{cn} \cdot C_{mac} \cdot \sqrt{A_{ap}}}{e^{C_{cp}}} + 9 \times 10^{-2} D_x^4 \cdot A_{cp} \cdot C_{ap} \cdot (A_{mac} + B_{mac}) + 3 \right] - 1.3 \times 10^{-4} \cos(A_{ap}) \cdot \cos(A_x) \cdot e^{B_{cn}} - 0.05 \cos(A_x) + 9 \frac{\frac{A_{ap} \times B_{ir} \times C_{ir}}{B_{cn} \times C_{mac} \times D_x^3} - 1.26}{\left( 3.1 \times 10^{-3} A_x \cdot (A_{mac} - C_{mac}) \cdot (4.6 \times 10^{-4} \frac{B_{cn} \cdot C_{mac} \cdot \sqrt{A_{ap}} \cdot A_{cp} \cdot C_{ap} \cdot (A_{mac} + B_{mac})}{D_{mac}^2} + 11 \right) + 1.4} \right\} + 1.4 \quad (1)$$

## 2, Prediction model of $\tau_f$ for quaternary materials:

$$\begin{aligned} \tau_f = & 11.17 \frac{(B_v + C_v) \cdot D_x \cdot A_v \cdot \varepsilon_r \cdot C_{ced}}{(A_{cp} + C_{cp}) \cdot C_{av}} + 44.92 \frac{(B_v + C_v) \cdot A_v \cdot D_x^2 \cdot \sin(A_{cn} \cdot A_{ir})}{A_{cp} + C_{cp}} + 1.69 \times \\ & 10^2 \frac{D_x \cdot [B_v + A_v \cdot \sin(B_{ir})]}{A_v \cdot (A_{cp} + C_{cp})} - \frac{364.72 \cdot D_x}{(A_{cp} + C_{cp})} - 1.5 \times 10^{-2} \frac{(B_{av} - C_{av}) \cdot (A_v + B_v) \cdot C_{ir} \cdot \varepsilon_r}{A_v} - 1.63 (B_{av} - \\ & C_{av}) \cdot C_{ir} - 4.44 \end{aligned} \quad (2)$$

### 3, Prediction model of $Q_f$ for quaternary materials:

$$Q_f = 1.2 \frac{B_{ap}}{B_{ap} + D_{ap}} \cdot \left\{ 3.7 \ln(B_{aw}) \cdot \left\{ 0.3 \frac{C_{cn}}{D_x \cdot C_{en}} \cdot \left[ 5.8 \times 10^5 \left( \frac{C_{cn} \cdot (B_x + C_x)}{B_{ap}^2 \cdot C_{en} \cdot B_{cn} \cdot \varepsilon_r} \right)^{\frac{1}{3}} + 27.9 C_{cn}^6 \cdot B_{ap}^6 \cdot C_{mac} - 4.7 \times 10^3 \right] + 3.5 \times 10^3 \frac{B_{en} \cdot |A_{en} - C_{en}|}{C_{ap}} + 135.1 \right\} + 1.5 \times 10^4 B_x \cdot A_{ir} \cdot B_{aw} \cdot \left( \frac{C_{cn}}{B_{ap} \cdot C_{en} \cdot \varepsilon_r} \right)^{\frac{1}{2}} \cdot \left( \frac{1}{C_{me}} \right)^{\frac{1}{3}} + 92.2 B_x \cdot A_{ir} \cdot B_{aw} - 4.2 \times 10^3 \right\} + 2.4 \times 10^6 \frac{B_x \cdot A_{cn}}{A_{ap}^6} - 1.5 \times 10^3 \quad (3)$$

#### 4, Prediction model of $\varepsilon_r$ for ternary materials:

$$\varepsilon_r = 0.76 \frac{A_{ir}}{\sin(A_{ir})} \left\{ 0.87 \frac{B_{mac}}{(B_{mac} + C_{mac})} \left\{ 0.973 \{ (0.3\sqrt{A_{cn}} - 4.7 \times 10^{-4} A_{mac} \cdot \sin(A_{mac})) [3.66 \times 10^{-4} B_{ap} \cdot B_{mac} \cdot B_{cp} \cdot (C_{cn} - A_{cn}) \cdot \cos(B_{cp}) + 8.3 \times 10^{-4} \frac{C_x \cdot A_{cn} \cdot A_{mac} \cdot A_{cp}^3}{A_{cp} + B_{cp}} + 6.26] + 2.9 \} + 1.6 \times 10^{-5} \frac{B_{mac} - A_{mac}}{A_x^3} + 0.19 \right\} + 3 \times 10^{-2} \{ 0.973 \{ (0.3\sqrt{A_{cn}} - 4.7 \times 10^{-4} A_{mac} \cdot \sin(A_{mac})) [3.66 \times 10^{-4} B_{ap} \cdot B_{mac} \cdot B_{cp} \cdot (C_{cn} - A_{cn}) \cdot \cos(B_{cp}) + 8.3 \times 10^{-4} \frac{C_x \cdot A_{cn} \cdot A_{mac} \cdot A_{cp}^3}{A_{cp} + B_{cp}} + 6.26] + 2.9 \} + 1.6 \times 10^{-5} \frac{B_{mac} - A_{mac}}{A_x^3} + 0.19 \right\} \right\}$$

$$10^{-5} \frac{B_{mac}-A_{mac}}{A_x^3} + 0.19 \Big\}^3 \frac{1}{|B_{mac}-C_{mac}|} + 2.87 \Big\} - 1.5 \times 10^{-4} \frac{B_{mac}}{A_x \cdot \cos(A_{ap})} + 1.08 \quad (4)$$

5, Prediction model of  $\tau_f$  for ternary materials:

$$\begin{aligned} \tau_f = & 1.09 \frac{B_{ap}}{B_{ap}+C_{ap}} \left\{ -0.33 B_{en} \cdot (B_{en} - C_{en}) \cdot \left\{ 0.75 \frac{A_{ced}}{\sin(A_{ced})} \left[ 4.1 \frac{1}{(A_v - C_v)} \cdot (-0.87 \times \right. \right. \right. \\ & \left. \left. \left. \frac{DK^3 \cdot \sin(A_v) \cdot \sin(B_v)}{B_{mac}} + 7.88 \times \frac{\cos|\sin(\varepsilon_r) - \sin(A_{cp})|}{C_x^3} \right) + 1.9 \times 10^{-3} \frac{B_{mac}-A_{mac}}{\cos(B_{en})} - 2.27 \right] + \right. \\ & \left. 1.89 \frac{B_{ap} \cdot B_{av}^3}{A_{mac}} + 3.06 \right\} - 0.14 \Big\} + 4.73 \times 10^{-2} \frac{|A_{mac}-B_{mac}|}{A_x} \div \left( -3.57 \frac{DK^3 \cdot \sin(A_v) \cdot \sin(B_v)}{B_{mac} \cdot (A_v - C_v)} + \right. \\ & \left. \left. 32.3 \frac{\cos|\sin(\varepsilon_r) - \sin(A_{cp})|}{C_x^3 \cdot (A_v - C_v)} - 3 \times 10^2 \frac{1}{A_v - C_v} + 1.9 \times 10^{-3} \frac{B_{mac}-A_{mac}}{\cos(B_{en})} - 2.27 \right) - 2.2 \quad (5) \right. \end{aligned}$$

6, Prediction model of  $Q_f$  for ternary materials:

$$\begin{aligned} Q_f = & 0.96 \frac{B_{me}}{B_{me}+C_{me}} \left\{ 1.02 \cos \left( e^{-\frac{C_{mac}}{\varepsilon_r}} \right) \cdot \left\{ 0.36 \frac{A_{cn}}{e^{A_{ir}}} [1.82 C_x \cdot (A_x + C_x) (9.13 \times \right. \right. \right. \\ & \left. \left. \left. 10^4 \left[ e^{-A_{ap}} + e^{-e^{-\frac{C_{mac}}{\varepsilon_r}}} \right] + 3.55 \frac{A_{cn} \cdot B_{cn}^2}{A_x \cdot A_{ir} \cdot (A_{me} + B_{me})} - 6.47 \times 10^4 \right) + 3.73 \times \right. \right. \\ & \left. \left. 10^4 \frac{B_{aw}}{A_{mac}(B_{ym} - A_{ym})} + 6.4 \times 10^2 \right] - 11.3 \frac{A_{me} \cdot B_{mac}}{A_{ir} \cdot B_{cn}} + 7.75 \times 10^3 \right\} + 1.04 \times \right. \\ & \left. 10^4 \sin(A_{ap}) \cdot \sin(B_{cn}) + 45.1 \right\} - 3.69 \times \\ & \left. \left. \left. 10^5 \frac{\cos \left( 9.13 \times 10^4 \left[ e^{-A_{ap}} + e^{-e^{-\frac{C_{mac}}{\varepsilon_r}}} \right] + 3.55 \frac{A_{cn} \cdot B_{cn}^2}{A_x \cdot A_{ir} \cdot (A_{me} + B_{me})} - 6.47 \times 10^4 \right) }{B_{me}^3} + 3.64 \times 10^2 \right) \quad (6) \right. \right. \right. \end{aligned}$$

**Supplementary Table 1. The associated features in these fitted models are presented in the table**

Index	Notation	Feature
1	ir	Ionic radius
2	ap	Atomic polarizability
3	cp	Chemical potential
4	cn	Coordinate number
5	mac	mass attenuation coefficient for CrK <sub>a</sub>
6	x	Normalized composition
7	ced	Core electron distance
8	v	Valence state
9	av	Atomic volume
10	aw	Atomic weight
11	ym	Young's modulus
12	me	melting enthalpy
13	en	Electronegativity